

Estimation of Fast Time-Varying Channels in OFDM Systems Using Two-Dimensional Prolate

F. Peña-Campos, Roberto Carrasco-Alvarez, O. Longoria-Gandara, and R. Parra-Michel

Abstract—Modern communication systems are based on orthogonal frequency division multiplexing (OFDM). They are designed for dealing with frequency selective channels considering invariance within the time-span of an OFDM symbol. However, this assumption is no longer valid when the transceivers operate in higher mobility scenarios or higher carrier frequencies. This condition provokes inter-carrier interference (ICI) that greatly degrades system performance. State-of-the-art approaches that satisfactorily mitigate this problem have a complexity of $\mathcal{O}(N^3)$, which makes them infeasible with current technology. In this paper, a novel channel estimation algorithm to cope with this problem is presented. It is based on a subspace approach using two-dimensional Prolate functions, achieving a complexity of only $\mathcal{O}(N^2)$. It depends only on the maximum delay spread and maximum Doppler spread while being robust in the sense that it is independent of the particular channel scattering function. Performance analysis of the proposed algorithm is presented. Simulation results under the WiMAX standard show that this algorithm improves previous results, achieving a bit error rate (BER) close to the one obtained with perfect channel state information (CSI) in very-fast transceiver mobility, as high as 874 Km/h over a 2.4 Ghz carrier frequency.

Index Terms—Basis expansion model, ICI mitigation, OFDM, time-varying channel estimation.

I. INTRODUCTION

ORTHOGONAL frequency division multiplexing (OFDM) has become a suitable modulation technique to transmit high data rates over frequency-selective channels because the estimation and equalization processes are simple over slow time-varying channels. In that environment, the channel variation for each OFDM symbol is negligible, which allows the fading in each subcarrier to be estimated and compensated independently [1]. However, incorporation of broadband applications in high-mobility devices as well as migration to higher carrier frequencies have made it necessary to deal with fast time-varying channels. In this scenario, a single OFDM symbol experiences channel variations and suffers inter-carrier interference (ICI) [2]. Since the ICI greatly impacts system performance [3], the estimation and compensation of the channel variation for each OFDM

symbol is crucial.

In order to deal with estimation of fast time-varying channels, several authors assume that variations of the channel impulse response (CIR) during an OFDM symbol can be approximated by a first-degree polynomial; thus, the CIR of a given OFDM symbol can be computed by performing a linear interpolation using the estimated CIR of its adjacent symbols, as in [4], [5] and [6]. In addition, [5] and [7] propose an iterative scheme that removes the ICI to pilots for the purpose of improving channel estimation. However, the use of linear interpolation is no longer appropriate when the channel's Doppler spread increases, leading to a high level of modeling error and degrading the channel estimate. Under these conditions, a basis expansion model (BEM) for the time variations of each tap is proposed in [8], [9], where the basis weights are estimated with the information in the pilots of the current OFDM symbol. These approaches consider the case where pilots are positioned using a cluster scheme (two or more pilots positioned consecutively in frequency [8] or time [9]), which is not supported by many of the OFDM communication standards. Extending this BEM approach, [10] estimates the weights by using pilots of the current OFDM symbol and its adjacent ones. In [11] a BEM is used together with Kalman filtering for estimating and tracking the channel's weights. Finally, in [12], an approach based on MMSE filter and predistortion is considered in line-of-sight (LOS) conditions, requiring knowledge of accurate channel statistics.

By analyzing the current algorithms, the following considerations can be highlighted:

- The number of physical paths in real channels may be very high or even infinite, as considered in several standards. In these scenarios, approaches [7], [11] are not directly applicable.
- In the case of channels with a finite number of physical paths, the delay estimations imply extra computational complexity. In addition, system performance can be largely degraded by small inaccuracies in the path gain and delay estimation, as shown in [11].
- Typically, mobile scenarios can not guarantee LOS. Besides, knowledge of accurate channel statistics implies both information that is hard to acquire or estimate and expensive signal processing, which makes approach [12] applicable only for particular scenarios.
- Since channel equalization is usually performed in the frequency domain (FD), and the channel variations are estimated in the time domain (TD), current approaches for dealing with ICI require performing a considerable number of Fourier transformations in order to obtain the channel estimate needed in the FD equalization.

Manuscript received May 4, 2012; revised September 14, 2012; accepted December 13, 2012. The associate editor coordinating the review of this paper and approving it for publication was S. Wei.

F. Peña-Campos and R. Parra-Michel are with the Department of Electrical Engineering, Communications Section, CINVESTAV-IPN, Guadalajara, Jalisco, 45019, Mexico (e-mail: {fpena, rparra}@gdl.cinvestav.mx).

R. Carrasco-Alvarez is with the Department of Electronic Engineering, University of Guadalajara-CUCEI, Guadalajara, Jalisco, 44430, Mexico (e-mail: roberto.carrasco@red.cucei.udg.mx).

O. Longoria-Gandara is with the Department of Electronics, Systems and IT, ITESO, Periferico Sur Manuel Gomez Morin 8585, 45604, Tlaquepaque, Jalisco, Mexico (e-mail: olongoria@iteso.mx).

This work was supported by CONACYT scholarship 234491 program, Mixbaal 158899 and CONACYT 181962 research grants.

Digital Object Identifier 10.1109/TWC.2013.010413.120624

- Finally, there is a trade-off between performance and complexity. Particularly, [11] yields the best reported performance at the expense of an $\mathcal{O}(N^3)$ complexity.

These considerations lead to the conclusion that it is desirable to find an estimation algorithm that has the following features:

- It must be independent of the number and delay-position of physical paths or their associated Doppler spectrum shapes.
- It must be capable of working in FD, in order to provide the channel estimate directly in a convenient format for the channel equalizer.
- It must provide a good performance at manageable computational complexity.

A. Objectives and Contributions

The aim and main contribution of this work is to provide an estimation algorithm that fulfills the foregoing requirements. The solution is based on a two-dimensional BEM for channel representation. Since the required information about channel statistics needs to be relaxed, here the approach exploited in [13]–[18] has been followed: only the maximum dispersion parameters are required to define a suitable two-dimensional basis for reduced parameter estimation and channel reconstruction. In addition, a large number of operations can be saved by using the BEM in FD, as in [15] and [17]. However, in contrast to these previous works that consider the channel expansion for an OFDM frame, in this paper, this proposal exploits the two-dimensional BEM for expanding the time-varying channel within an OFDM symbol. The resulting algorithm has a manageable complexity of $\mathcal{O}(N^2)$ with a slight improvement in system performance when compared with the best results of previous approaches.

B. Notation

Bold lower (upper) case letters are used to denote vector (matrices); $(\cdot)^T$, $(\cdot)^H$ and $\lceil \cdot \rceil$ denote transpose, Hermitian and round up operators, respectively; $(\cdot)^{(t)}$ denotes vectors or matrices in time domain, otherwise it indicates frequency domain; $(\cdot)^{(n)}$ denotes that the n -th OFDM symbol is considered; $\langle \cdot \rangle_N$ denotes a circular shift modulus N ; $E\{\cdot\}$ is the expected value and $\text{tr}\{\cdot\}$ denotes the matrix trace. Subscripts $(\cdot)_p$ and $(\cdot)_d$ denote the sampled version at pilot and/or data positions in vectors, and the sampled version at pilot and/or data rows and columns in matrices. $[\mathbf{H}]_{k,l}$ denotes the l -th element in the k -th row of matrix \mathbf{H} . \mathbf{R}_a and $\mathbf{R}_{a,b}$ denote the autocorrelation matrix of \mathbf{a} , and the correlation matrix between \mathbf{a} and \mathbf{b} .

C. Organization

This paper is organized as follows: Section II describes the time-varying channel and the OFDM system models. Section III explains the two-dimensional BEM and the derivation of the proposed algorithm. The performance analysis of the introduced estimator is presented in Section IV, while its computational complexity is discussed in Section V. Simulation results are illustrated in Section VI. Finally, in Section VII the conclusions are stated.

II. SYSTEM MODEL

Let $x^{(t,n)}(k)$ be the n -th transmitted OFDM symbol in the time domain that is made up of N samples, where $N = N_b - N_g$ is the discrete Fourier transform (DFT) size, N_g is the cyclic prefix (CP) length and N_b is the OFDM symbol length including CP. Assuming that CP is large enough to avoid intersymbol interference (ISI), the received symbol in the time domain, $y^{(t,n)}(k)$, after CP removal, can be expressed in the complex baseband representation (hereafter considered in this paper) as:

$$y^{(t,n)}(k) = \sum_{l=0}^{L-1} h^{(n)}(k, l) x^{(t,n)}(\langle k - l \rangle_N) + w^{(t,n)}(k), \quad (1)$$

where $k = (0, \dots, N-1)$, $k' = (0, \dots, N-1)$, $l = (0, \dots, L-1)$. $L = \lceil \tau_{max}/T_{samp} \rceil$ is the baseband CIR length, τ_{max} is the maximum delay spread and T_{samp} is the sampling period. $h^{(n)}(k, l)$ is the time-varying CIR corresponding to the n -th symbol at instant k for an impulse introduced l samples previously; $w^{(t,n)}(k)$ is the additive white Gaussian noise. Thus, (1) represents the circular convolution between the CIR and $x^{(t,n)}(k)$, which can be expressed in matrix form as:

$$\mathbf{y}^{(t,n)} = \mathbf{H}^{(n)} \mathbf{x}^{(t,n)} + \mathbf{w}^{(t,n)} \quad (2)$$

where

$$\begin{aligned} \mathbf{y}^{(t,n)} &= \begin{bmatrix} y^{(t,n)}(0) & y^{(t,n)}(1) & \dots & y^{(t,n)}(N-1) \end{bmatrix}^T, \\ \mathbf{x}^{(t,n)} &= \begin{bmatrix} x^{(t,n)}(0) & x^{(t,n)}(1) & \dots & x^{(t,n)}(N-1) \end{bmatrix}^T, \\ \mathbf{w}^{(t,n)} &= \begin{bmatrix} w^{(t,n)}(0) & w^{(t,n)}(1) & \dots & w^{(t,n)}(N-1) \end{bmatrix}^T \end{aligned}$$

is an additive white circularly symmetric complex Gaussian noise vector, with zero mean and variance $\sigma_w^2 = N_0/2$. In addition, $\mathbf{H}^{(n)}$ is an $N \times N$ matrix whose elements are formed with the CIR coefficients as follows:

$$[\mathbf{H}^{(n)}]_{k,k'} = h^{(n)}(k, \langle k - k' \rangle_N), \quad (3)$$

where $k, k' = (0, 1, \dots, N-1)$ and CIR is assumed to be zero for $\langle k - k' \rangle_N > L-1$. In order to simplify the reading, hereafter the term OFDM symbol refers to the OFDM symbol excluding the CP. Defining the normalized DFT matrix as:

$$[\mathbf{F}]_{k,k'} = \frac{1}{\sqrt{N}} e^{-j2\pi k k' / N}, \quad (4)$$

the received OFDM symbol in the FD is obtained by premultiplying both sides of (2) by (4), which results in

$$\mathbf{y}^{(n)} = \mathbf{F} \mathbf{H}^{(n)} \mathbf{x}^{(t,n)} + \mathbf{w}^{(n)}, \quad (5)$$

where $\mathbf{y}^{(n)}$ is the received OFDM symbol in the FD and $\mathbf{w}^{(n)}$ is the DFT of noise sequence. Since matrix \mathbf{F} has the properties $\mathbf{F}^{-1} = \mathbf{F}^H$ and $\mathbf{F}^H \mathbf{F} = \mathbf{I}$, where \mathbf{I} is the identity matrix of size $N \times N$, (5) can be expressed as:

$$\begin{aligned} \mathbf{y}^{(n)} &= \mathbf{F} \mathbf{H}^{(n)} \mathbf{F}^H \mathbf{F} \mathbf{x}^{(t,n)} + \mathbf{w}^{(n)}, \\ &= \mathbf{F} \mathbf{H}^{(n)} \mathbf{F}^H \mathbf{x}^{(n)} + \mathbf{w}^{(n)}, \\ &= \mathbf{G}^{(n)} \mathbf{x}^{(n)} + \mathbf{w}^{(n)}; \end{aligned} \quad (6)$$

where $\mathbf{G}^{(n)} = \mathbf{F} \mathbf{H}^{(n)} \mathbf{F}^H$ is the channel frequency matrix (CFM). Eq. (6) models the received OFDM symbol $\mathbf{y}^{(n)}$ as

a linear transformation of the transmitted symbol in the FD, $\mathbf{x}^{(n)}$ and the CFM. It is important to point out that CFM is the frequency and frequency-Doppler information of a circular and sparse representation of the time-varying CIR. As highlighted in [2], when the Doppler spread is negligible, $\mathbf{G}^{(n)}$ is diagonal and the system is ICI-free. On the other hand, when the Doppler spread is significant, the matrix becomes banded, inducing ICI.

III. ESTIMATION ALGORITHM

A. Two-Dimensional Basis Expansion Model

The time-varying CIR can be modeled as a weighted sum of two-dimensional basis functions as:

$$h^{(n)}(k, l) = \sum_{i=1}^I \rho_i \phi_i(k, l) + \varepsilon_m(k, l) \quad (7)$$

where ρ_i is the weighting factor of the $\phi_i(k, l)$ base function, I is the number of basis functions to be used and ε_m is the modeling error since some base functions were dismissed, i.e., $0 < I < N^2$. Based on the procedures described in [15], [18], in this work the two-dimensional basis functions $\phi_i(k, l)$ that expand the channel variations within the OFDM symbol are constructed as the outer product of two one-dimensional functions, i.e.:

$$\phi_i(k, l) = v_r(k) \gamma_q(l), \quad (8)$$

where $i = q + Q(r - 1)$, $1 \leq r \leq R$, and $1 \leq q \leq Q$. The numbers Q and R refer to the basis functions used in time-delay and time domains, respectively. Each basis spans a particular dimension: $\gamma_q(l)$ spans the time-delay domain while $v_r(k)$ spans the time domain.

The choice of the foregoing bases is made with partial knowledge of channel statistics; otherwise (with complete knowledge of channel statistics) the Karhunen-Loève expansion (KLE) would be the natural option. Moreover, the correlation function of the time-varying channel depends on four variables, but assuming knowledge of only the maximum Doppler and delay spread as well as system parameters, the resulting channel kernel can be decomposed as the external product of two independent Prolate kernels (see [13], [15] and [18] for details). Hence, the two-dimensional Prolate basis used in the proposed approach is optimal in the sense of being the eigenfunctions of a kernel with partial but realistic channel information. Note that the estimator proposed in [13] is completely different from the one proposed here, i.e., the basis in [13] is not two-dimensional prolate and the system is single carrier with superimposed training. It is also important to clarify that even though [17] and [15] deal with double selective channels in OFDM systems using two-dimensional prolate, they assume that the CIR is invariant during the OFDM symbol period, allowing only intra-frame variations. This assumption leads to a simplified model which cannot deal with ICI. Thus, it can be observed that channel impairments, estimator objectives and the estimation algorithm presented in this paper are totally different from the ones discussed in [17] [13] and [15].

It is well-known that discrete prolate spheroidal sequences (DPSS) are discrete functions that concentrate most of the

energy in finite time and bandwidth windows [19]. Their computation requires only knowledge of the maximum time T and bandwidth B_w . In the case of an OFDM system over a time-varying channel, it is necessary to compute two separate DPSS bases, one for expanding the time-delay domain and the other for the time domain. The parameters associated with the time-delay DPSS are the effective bandwidth B (i.e., the symbol bandwidth without guard bands) and the maximum channel delay spread τ_{max} . For the time domain, the parameters are the maximum Doppler spread ν_{max} and the OFDM symbol period T_S .

DPSS's for the time dimension can be computed as the solution to [19]:

$$\sum_{k'_{Nb}=1}^{N_b} \frac{\sin(2\pi\nu_{max}T_S(k'_{Nb} - k_{Nb}))}{\pi(k'_{Nb} - k_{Nb})} v_r(k'_{Nb}) = \lambda_r v_r(k_{Nb}), \quad (9)$$

and the DPSS's for the time-delay dimension are obtained by solving:

$$\sum_{l'=1}^L \frac{\sin(\pi B \tau_{max}(l' - l))}{\pi(l' - l)} \gamma_q(l') = \lambda_q \gamma_q(l), \quad (10)$$

where $k_{Nb}, k'_{Nb} = (1, 2, \dots, N_b)$ and $l, l' = (1, 2, \dots, L)$; λ_r and λ_q are the eigenvalues associated with $v_r(k)$ and $\gamma_q(l)$ respectively. In [19] it is established that the number of necessary sequences to collect most of the process energy is given by $\lceil B_w T \rceil + 1$. Thus, the approximated dimensionality of the basis to be used at each domain is:

$$Q = \lceil B \tau_{max} \rceil + 1, \quad (11)$$

$$R = \lceil 2\nu_{max} T_S \rceil + 1. \quad (12)$$

In this way, the number of necessary functions of the two-dimensional basis for expanding the time-variant CIR can be known in advance and computed as:

$$I = (\lceil B \tau_{max} \rceil + 1) (\lceil 2\nu_{max} T_S \rceil + 1). \quad (13)$$

Note that current approaches for combating ICI use a BEM for the channel only in the time domain. In this work, a BEM is also performed in the FD; this allows a reduction in the number of parameters to be estimated, as the dimensionality Q in this domain (which is equivalent in dimensionality for expanding the time-delay domain) is reduced by discriminating guard bands in the BEM. The resulting number of required parameters for time-delay expansion will be generally lower than the number of taps in the discrete channel representation, and independent of the number and delay of the physical paths. Therefore, this improvement achieved by the proposed two-dimensional BEM represents an advantage for channel estimation that is independent of the particular weight estimator to be considered.

B. Weight Estimation

In most communication standards based on OFDM (such as WiMAX, LTE, Wi-Fi, etc.) training is included at each OFDM data symbol. N_p subcarriers called pilots are distributed along the used bandwidth and modulated with values known by the receiver. But the information contained

in the pilots of a single OFDM symbol only provides an average of the channel transfer function within the time interval corresponding to this symbol. Thus, in order to estimate the channel time-varying response, it is necessary to work with more than one OFDM symbol, i.e., averages of different time intervals. In this work the weight estimation is performed using the pilots of the current OFDM symbol and N_S adjacent ones where:

$$N_S = N_L + N_R, \quad (14)$$

N_L is the number of previous adjacent symbols and N_R is the number of posterior adjacent symbols. Hereafter, the current OFDM symbol refers to the OFDM symbol whose CFM is being estimated. By using (2), the array of the current OFDM symbol and its adjacent ones can be expressed as:

$$\begin{bmatrix} \mathbf{y}^{(t, n-N_L)} \\ \vdots \\ \mathbf{y}^{(t, n)} \\ \vdots \\ \mathbf{y}^{(t, n+N_R)} \end{bmatrix} = \begin{bmatrix} \mathbf{H}_{n-1} \mathbf{x}^{(t, n-N_L)} \\ \vdots \\ \mathbf{H}_n \mathbf{x}^{(t, n)} \\ \vdots \\ \mathbf{H}_{n+1} \mathbf{x}^{(t, n+N_R)} \end{bmatrix} + \begin{bmatrix} \mathbf{w}^{(t, n-N_L)} \\ \vdots \\ \mathbf{w}^{(t, n)} \\ \vdots \\ \mathbf{w}^{(t, n+N_R)} \end{bmatrix}. \quad (15)$$

In order to apply the BEM to (15), the two-dimensional base is extended to span $N_S + 1$ OFDM symbol periods, i.e., the time domain basis $v_r(k)$ is extended to cover $N_S + 1$ symbols including their corresponding CP intervals. This condition implies that computation of $v_r(k)$ is the solution to

$$\sum_{k'_e=1}^{(N_S+1)N_b} \frac{\sin(2\pi f_D(N_S+1)(k'_e - k_e))}{\pi(k'_e - k_e)} v_r(k'_e) = \lambda_r v_r(k_e), \quad (16)$$

where $f_D = \nu_{max} T_S$ is the normalized Doppler frequency, $k_e, k'_e = (1, 2, \dots, (N_S + 1)N_b)$. The number of necessary functions to expand the extended time-Doppler domain for three symbols, R_{ext} , results in:

$$R_{ext} = \lceil 2\nu_{max}(N_S + 1)T_S \rceil + 1. \quad (17)$$

Hence, each two-dimensional basis function is now $(N_S + 1)N_b \times L$ in size. The basis functions need to be partitioned in order to expand the corresponding part of each OFDM symbol interval without the CP in (15). Therefore partitions of size $N \times N$ are defined as:

$$\begin{aligned} \phi_i^{(n-N_L)}(k, k') &= v_r(N_g + k) \gamma_q(k'), \\ \phi_i^{(n-N_L+1)}(k, k') &= v_r(N_b + N_g + k) \gamma_q(k'), \\ &\vdots \\ \phi_i^{(n)}(k, k') &= v_r(N_L N_b + N_g + k) \gamma_q(k'), \\ &\vdots \\ \phi_i^{(n+N_R)}(k, k') &= v_r(N_S N_b + N_g + k) \gamma_q(k'), \end{aligned} \quad (18)$$

where $\gamma_q(k') = 0$ for $k' \geq L$. Using the previous expression, each received OFDM symbol in the array of (15) can be

represented as:

$$\mathbf{y}^{(t, n-n')} = \sum_{i=1}^I \rho_i \Phi_i^{(n-n')} \mathbf{x}^{(t, n-n')} + \Xi^{(n-n')} \mathbf{x}^{(t, n-n')} + \mathbf{w}^{(t, n-n')}, \quad (19)$$

where $n' = (N_L, N_L - 1, \dots, 0, \dots, -N_R + 1, -N_R)$, $\Xi^{(n)}$ is the matrix of modeling error and $\Phi_i^{(n)}$ is a matrix of size $N \times N$ with the coefficients in the form

$$[\Phi_i^{(n)}]_{k, k'} = \phi_i^{(n)}(k, \langle k - k' \rangle_N). \quad (20)$$

Note that $\Phi_i^{(n)}$ is nothing but the arrangement of the basis coefficients in way that represents the time variant channel and signal convolution in a matrix-vector form, as in (3). Applying the same procedure as in (6), the frequency domain expression of (19) is:

$$\mathbf{y}^{(n-n')} = \sum_{i=1}^I \rho_i \Theta_i^{(n-n')} \mathbf{x}^{(n-n')} + \xi^{(n-n')} + \mathbf{w}^{(n-n')}, \quad (21)$$

where

$$\Theta_i^{(n)} = \mathbf{F} \Phi_i^{(n)} \mathbf{F}^H \quad (22)$$

are the partitioned basis functions for the CFM and

$$\xi^{(n)} = \mathbf{F} \Xi^{(n)} \mathbf{F}^H \mathbf{x}^{(n)} \quad (23)$$

is the ICI that is not spanned by the reduced basis (i.e., the ICI contained in the modeling error).

Let $\mathbf{x}_p^{(n)}$ and $\mathbf{y}_p^{(n)}$ be vectors of size N_p with the elements of $\mathbf{x}^{(n)}$ and $\mathbf{y}^{(n)}$ at pilot positions, respectively, and $\Theta_{i,p}^{(n)}$ be the submatrix of size $N_p \times N_p$ formed with the columns and rows of $\Theta_i^{(n)}$ corresponding to the pilot positions. Thus, the received signal at pilot positions is obtained by sampling (21), leading to:

$$\mathbf{y}_p^{(n-n')} = \sum_{i=1}^I \rho_i \Theta_{i,p}^{(n-n')} \mathbf{x}_p^{(n-n')} + \xi_p^{(n-n')} + \mathbf{q}^{(n-n')} + \mathbf{w}_p^{(n-n')}, \quad (24)$$

where the term $\mathbf{q}^{(n-n')}$ contains the ICI in pilots induced by data subcarriers, and the terms $\xi_p^{(n-n')}$ and $\mathbf{w}_p^{(n-n')}$ are the sampled versions of $\xi^{(n-n')}$ and $\mathbf{w}^{(n-n')}$ at pilot positions. Since $\mathbf{x}_p^{(n)}$ and $\Theta_{i,p}^{(n)}$ are known by the receiver, their product, $\Lambda^{(n)}$ can be precomputed and stored. Therefore, (24) can be rewritten as:

$$\mathbf{y}_p^{(n-n')} = \Lambda^{(n-n')} \boldsymbol{\rho} + \xi_p^{(n-n')} + \mathbf{q}^{(n-n')} + \mathbf{w}_p^{(n-n')} \quad (25)$$

where,

$$\Lambda^{(n)} = \begin{bmatrix} \Theta_{1,p}^{(n)} \mathbf{x}_p^{(n)} & \Theta_{2,p}^{(n)} \mathbf{x}_p^{(n)} & \dots & \Theta_{I,p}^{(n)} \mathbf{x}_p^{(n)} \end{bmatrix} \quad (26)$$

is a matrix of size $N_p \times I$ and $\boldsymbol{\rho} = [\rho_1 \ \rho_2 \ \dots \ \rho_I]^T$ is the vector of basis weights to be estimated. Gathering (25) for the three received OFDM symbols at pilot positions in a

single array results in:

$$\begin{bmatrix} \mathbf{y}_p^{(n-N_L)} \\ \vdots \\ \mathbf{y}_p^{(n)} \\ \vdots \\ \mathbf{y}_p^{(n+N_R)} \end{bmatrix} = \begin{bmatrix} \mathbf{\Lambda}^{(n-N_L)} \\ \vdots \\ \mathbf{\Lambda}^{(n)} \\ \vdots \\ \mathbf{\Lambda}^{(n+N_R)} \end{bmatrix} \boldsymbol{\rho} + \begin{bmatrix} \boldsymbol{\epsilon}_p^{(n-N_L)} \\ \vdots \\ \boldsymbol{\epsilon}_p^{(n)} \\ \vdots \\ \boldsymbol{\epsilon}_p^{(n+N_R)} \end{bmatrix}, \quad (27)$$

where

$$\boldsymbol{\epsilon}_p^{(n-n')} = \boldsymbol{\xi}_p^{(n-n')} + \boldsymbol{\varrho}^{(n-n')} + \mathbf{w}_p^{(n-n')}. \quad (28)$$

Defining

$$\begin{aligned} \mathbf{\Lambda}^T &= \begin{bmatrix} \mathbf{\Lambda}^{(n-N_L)T} & \dots & \mathbf{\Lambda}^{(n)T} & \dots & \mathbf{\Lambda}^{(n+N_R)T} \end{bmatrix}^T, \\ \mathbf{y}_p &= \begin{bmatrix} \mathbf{y}_p^{(n-N_L)T} & \dots & \mathbf{y}_p^{(n)T} & \dots & \mathbf{y}_p^{(n+N_R)T} \end{bmatrix}^T, \\ \boldsymbol{\epsilon}_p &= \begin{bmatrix} \boldsymbol{\epsilon}_p^{(n-N_L)T} & \dots & \boldsymbol{\epsilon}_p^{(n)T} & \dots & \boldsymbol{\epsilon}_p^{(n+N_R)T} \end{bmatrix}^T, \end{aligned}$$

then the expression for the array of received pilots can be laconically rewritten as:

$$\mathbf{y}_p = \mathbf{\Lambda} \boldsymbol{\rho} + \boldsymbol{\epsilon}_p. \quad (29)$$

By analyzing the terms that conform (28), it is possible to observe that vector $\boldsymbol{\epsilon}_p$ is made up of a linear combination of many zero-mean uncorrelated random variables (ICI from data subcarriers, channel response, modeling error and additive noise); thus, by applying the central limit theorem it is possible to assume that elements of $\boldsymbol{\epsilon}_p$ are zero-mean Gaussian variables. Considering the foregoing and that weights statistics are unavailable, the computation of the weight estimate via the least squares (LS) algorithm [20] is an adequate approach, leading to:

$$\hat{\boldsymbol{\rho}} = (\mathbf{\Lambda}^H \mathbf{\Lambda})^{-1} \mathbf{\Lambda}^H \mathbf{y}_p = \boldsymbol{\Gamma} \mathbf{y}_p \quad (30)$$

where $\hat{\boldsymbol{\rho}}$ is the weight estimate vector and $\boldsymbol{\Gamma} = (\mathbf{\Lambda}^H \mathbf{\Lambda})^{-1} \mathbf{\Lambda}^H$. Note that the model proposed in this paper makes it possible to consider any other algorithm as the minimum mean squared error (MMSE); for instance, the reduced rank approximation presented in [14] can be used.

It is important to highlight that matrix $\boldsymbol{\Gamma}$ is $I \times (N_S + 1)N_p$ in size and made up of the basis and pilot information; it can therefore be precomputed and stored at the receiver. In addition, the proposed algorithm is robust in the sense that Doppler spectrum and delay-profile shapes are not required, and independent of the number of physical paths.

C. Channel reconstruction

The channel reconstruction consists of the weighting of the basis functions using the estimated weights. Since only the channel estimate of the current OFDM symbol is needed by the equalizer, the reconstruction step requires only the partition corresponding to that symbol. This can be performed in TD, leading to the CIR estimate:

$$\hat{\mathbf{H}}^{(n)} = \sum_{i=1}^I \hat{\rho}_i \boldsymbol{\Phi}_i^{(n)}. \quad (31)$$

If the equalization is performed in FD, it is advisable to reconstruct the CFM estimate as:

$$\hat{\mathbf{G}}^{(n)} = \sum_{i=1}^I \hat{\rho}_i \boldsymbol{\Theta}_i^{(n)}. \quad (32)$$

Note that basis functions can be stored in the TD form ($\boldsymbol{\Phi}_i^{(n)}$) or in the FD domain form ($\boldsymbol{\Theta}_i^{(n)}$); thus no transformations are needed for estimation in runtime.

D. Iterative scheme

The estimation is carried out with the information contained in the pilots; but initially, these pilots are distorted by the ICI coming from data subcarriers as well as the additive noise, which impacts the algorithm performance. As in [11], an alternative to overcome this drawback consists of using an estimated channel for equalization and data estimation. Then, data is passed through the estimated channel, which provides an approximation of the induced ICI in the pilot positions. The estimated ICI is subtracted from the received symbol at pilot positions. Thus, data-ICI is reduced in pilots, which allows for better channel estimation. This process can be executed iteratively in order to improve the channel estimation and data detection. Mathematically, the procedure expressed above can be written as:

$$\mathbf{y}^{(it,n)} = \mathbf{y}^{(it-1,n)} - \hat{\mathbf{G}}^{(it-1,n)} \mathbf{z}^{(it-1,n)}, \quad (33)$$

where the superscript $it = 1, 2, \dots$ denotes the iteration number. $\mathbf{y}^{(0,n)}$ is the n -th received OFDM symbol, $\hat{\mathbf{G}}^{(it-1,n)}$ is the estimated channel in the past iteration, and $\mathbf{z}^{(it-1,n)}$ is an OFDM symbol constructed from the estimated data in the previous iteration and zeros in the pilot positions. In this manner, as the channel estimate becomes better, the induced ICI in pilots from data subcarriers can be reduced, improving system performance.

IV. PERFORMANCE ANALYSIS

A. Bias

For performance analysis, the bias of the channel estimate and the covariance matrix of the estimated weights are carried out. The bias in FD can be defined as follows:

$$\text{bias}[\hat{\mathbf{G}}^{(n)}] = E\{\hat{\mathbf{G}}^{(n)}\} - \mathbf{G}^{(n)}. \quad (34)$$

The BEM model in (21) and (32) allows (34) to be expressed as:

$$\begin{aligned} \text{bias}[\hat{\mathbf{G}}^{(n)}] &= E\left\{\sum_{i=1}^I \hat{\rho}_i \boldsymbol{\Theta}_i^{(n)}\right\} - \left(\sum_{i=1}^I \rho_i \boldsymbol{\Theta}_i^{(n)} + \mathbf{F} \boldsymbol{\Xi}^{(n)} \mathbf{F}^H\right) \\ &= \sum_{i=1}^I E\{\hat{\rho}_i\} \boldsymbol{\Theta}_i^{(n)} - \left(\sum_{i=1}^I \rho_i \boldsymbol{\Theta}_i^{(n)} + \mathbf{F} \boldsymbol{\Xi}^{(n)} \mathbf{F}^H\right). \end{aligned} \quad (35)$$

Since the ICI, noise and channel are all zero-mean random processes, the weight estimation provided by the LS algorithm is unbiased, therefore:

$$\begin{aligned} \text{bias}[\hat{\mathbf{G}}^{(n)}] &= \sum_{i=1}^I \rho_i \boldsymbol{\Theta}_i^{(n)} - \left(\sum_{i=1}^I \rho_i \boldsymbol{\Theta}_i^{(n)} + \boldsymbol{\epsilon}_m\right) \\ &= -\mathbf{F} \boldsymbol{\Xi}^{(n)} \mathbf{F}^H. \end{aligned} \quad (36)$$

Since bias in (36) is determined by the modeling error, the proposed estimator can be considered unbiased when the employed reduced basis collects most of the process energy.

B. Covariance Matrix

The weight estimator covariance matrix, $\mathbf{R}_{\hat{\rho}}$, can be obtained as

$$\begin{aligned}\mathbf{R}_{\hat{\rho}} &= E \left\{ (\hat{\rho} - E[\hat{\rho}]) (\hat{\rho} - E[\hat{\rho}])^H \right\} \\ &= E \left\{ \hat{\rho} \hat{\rho}^H - \hat{\rho} E\{\hat{\rho}\}^H - E\{\hat{\rho}\} \hat{\rho}^H + E\{\hat{\rho}\} E\{\hat{\rho}\}^H \right\}.\end{aligned}\quad (37)$$

Substituting the estimator expression (30) in (37) and noting that the actual and estimated weights are zero mean, it follows that:

$$\mathbf{R}_{\hat{\rho}} = \mathbf{\Gamma} \mathbf{R}_{\mathbf{y}_p} \mathbf{\Gamma}^H. \quad (38)$$

As (38) shows, the covariance of estimated weights depends directly on the covariance of the received pilots, which is computed as:

$$\mathbf{R}_{\mathbf{y}_p} = E \left\{ (\mathbf{\Lambda} \rho + \boldsymbol{\xi}_p + \boldsymbol{\varrho} + \mathbf{w}_p) (\mathbf{\Lambda} \rho + \boldsymbol{\xi}_p + \boldsymbol{\varrho} + \mathbf{w}_p)^H \right\} \quad (39)$$

Expanding (39) and omitting the cross-correlation terms with zero values because of the channel and data decorrelation results in:

$$\mathbf{R}_{\mathbf{y}_p} = \mathbf{\Lambda} \mathbf{R}_{\rho} \mathbf{\Lambda}^H + \mathbf{R}_{\boldsymbol{\xi}_p} + \mathbf{R}_{\boldsymbol{\varrho}} + \mathbf{R}_{\mathbf{w}_p} + \mathbf{R}_{\boldsymbol{\xi}_p, \mathbf{\Lambda} \rho} + \mathbf{R}_{\mathbf{\Lambda} \rho, \boldsymbol{\xi}_p}, \quad (40)$$

where the cross-correlation terms $\mathbf{R}_{\mathbf{\Lambda} \rho, \boldsymbol{\xi}_p}$ and $\mathbf{R}_{\boldsymbol{\xi}_p, \mathbf{\Lambda} \rho}$ cannot be assumed as zero-value matrices since the modeling error is not decorrelated with the channel weights (this assumption applies only to the Karhunen-Loève basis [21] where each base function is an eigenfunction of the process) and pilots have constant values. Substituting (40) in (38) yields the covariance matrix of the estimated weights:

$$\mathbf{R}_{\hat{\rho}} = \mathbf{R}_{\rho} + \mathbf{\Gamma} (\mathbf{R}_{\boldsymbol{\xi}_p} + \mathbf{R}_{\boldsymbol{\varrho}} + \mathbf{R}_{\mathbf{w}_p} + \mathbf{R}_{\boldsymbol{\xi}_p, \mathbf{\Lambda} \rho} + \mathbf{R}_{\mathbf{\Lambda} \rho, \boldsymbol{\xi}_p}) \mathbf{\Gamma}^H. \quad (41)$$

C. Mean squared error

Mean squared error for the weight estimate can be expressed as [20]:

$$\begin{aligned}\text{MSE} &= \text{tr} \left\{ E \left\{ (\hat{\rho} - \rho) (\hat{\rho} - \rho)^H \right\} \right\} \\ &= \text{tr} \left\{ \mathbf{\Gamma} (\mathbf{R}_{\boldsymbol{\xi}_p} + \mathbf{R}_{\boldsymbol{\varrho}}) \mathbf{\Gamma}^H \right\} + \sigma_w^2 \text{tr} \left\{ (\mathbf{\Lambda}^H \mathbf{\Lambda})^{-1} \right\}\end{aligned}\quad (42)$$

From (42), it is clear that the performance of the proposed algorithm depends on the modeling error through $\mathbf{R}_{\boldsymbol{\xi}_p}$, and explains the impact of selecting an adequate number of basis functions. The ICI is present in the term $\mathbf{R}_{\boldsymbol{\varrho}}$, which can be reduced by means of the iterative scheme.

V. COMPUTATIONAL COMPLEXITY

The computational complexity of the proposed algorithm is summarized in Table I. As mentioned earlier, the algorithm consists of two steps: weight estimation and channel reconstruction. The weight estimation is computed by using (30), which is a matrix-vector product that requires $(N_S + 1)R_{ext}QN_p$ complex multiplications. In practice, the number of required basis functions I and the number of pilots per

TABLE I
COMPUTATIONAL COMPLEXITY OF PROPOSED ALGORITHM

Computation step	Number of required products	
Weight estimation	$(N_S + 1)IN_p$	
Channel reconstruction	TD	FD
	$QR_{ext}LN$	$QR_{ext}N_DN$
Total	$QR_{ext}((N_S + 1)N_p + LN)$	$QR_{ext}((N_S + 1)N_p + N_DN)$

TABLE II
COMPUTATIONAL COMPLEXITY COMPARISON

Work	Computational complexity	Order
[11]	$2N^3 + -2N^2 + N + N(N_pLR_{ext})^2 + NLR_{ext}(N_p - 1)(N + LR_{ext} + 1) + N_pLR_{ext}^2 + N^2(R_{ext} - 1) + NLR_{ext} + N^2L(R_{ext} - 1) + NL$	$\mathcal{O}(N^3)$
Proposed FD	$QR_{ext}((N_S + 1)N_p + N_DN)$	$\mathcal{O}(N^2)$

OFDM data symbol N_p are lower than N , and one adjacent symbol at each side is enough to obtain good performance. For these reasons, the complexity of weight estimation is much lower than $\mathcal{O}(N^2)$.

The channel reconstruction can be computed in TD with (31) or in FD with (32). Because in TD the channel matrix has just L non-zero elements per row, the cost of weighting each base is LN complex products; therefore, computation of (31) requires a total of $QR_{ext}LN$ products. In FD, the CFM $\mathbf{G}^{(n)}$ is a diagonal dominant matrix with most of the energy concentrated on the main diagonals [2], which makes it possible to dismiss far diagonal elements and approximate it as a sparse matrix with N_D non-zero diagonals. Therefore, computation of (32) can be performed with $QR_{ext}N_DN$ products.

Table II shows a comparison of the computational complexity between the proposed work and approach presented in [11]. The number of complex products corresponds only to the channel estimation and does not involve ICI mitigation or equalization. It is worth mentioning that approaches in [10], [11] also require the estimation of the path delays, whose complexity is not included in the comparison. Note that the computational load required by the proposed algorithm is low since the growth order was reduced from $\mathcal{O}(N^3)$ [11] to $\mathcal{O}(N^2)$. Complexity of the iterative algorithm for data-ICI mitigation as well as for equalization is the same as the one presented in [11].

The flexibility of computing the channel estimate in any domain (TD or FD) through a BEM results in a channel estimation algorithm with the following features:

- The computational complexity of the proposed algorithm including channel matrix reconstruction at any domain is $\mathcal{O}(N^2)$, which is lower than the complexity of the state-of-the-art algorithms.
- As in [15] and [17], the use of a two-dimensional BEM allows the proposed algorithm to provide the channel estimate matrix at FD or TD directly, without requiring the computation of the exhaustive transformation $\mathbf{G}^{(n)} = \mathbf{F}\mathbf{H}^{(n)}\mathbf{F}^H$ that is usually performed with several FFT's. This represents an important advantage over other BEM

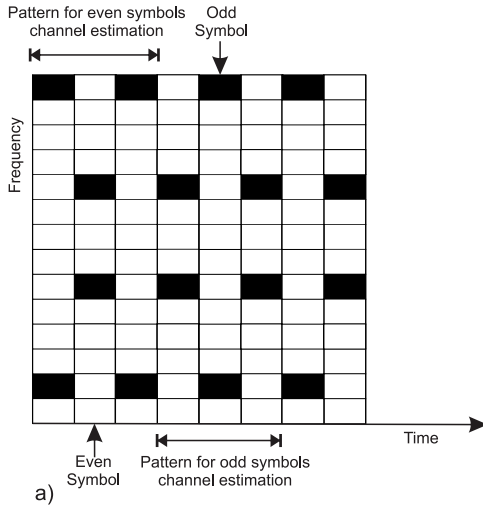


Fig. 1. Pilot pattern specified in the IEEE 802.16e communication standard also known as mobile WiMAX. The black squares represent pilot subcarriers while the white squares represent data subcarriers. The proportion of pilot subcarriers is $1/7$ or $N_p = 60$ pilots.

- approaches such as [8], [10], [11] and [9] that represent each physical or discrete channel tap independently.
- Since the proposed method does not require path-delay estimation, latency is reduced to only one OFDM symbol, in contrast to [11].
 - The 2D-prolate basis allows the algorithm to be independent of the particular channel scattering function.

VI. SIMULATION RESULTS

The algorithm was tested and compared in an 802.16e downlink (mobile WiMAX) simulation environment with a multipath Rayleigh channel. The system parameters are: $N = 512$, $N_G = \frac{1}{8}N$, $T_s = 102.857\mu s$, sampling frequency $F_s = 5.6$ Mhz, $N_L = 1$, $N_R = 1$ and unitary power 4-QAM as data constellation. Considering 90 subcarriers as guard bands, effective bandwidth is $B = 4.61$ Mhz. In order to present the raw bit error rate (BER) that can be obtained with this approach, the forward error correction scheme is not included.

Two pilot arrangements are considered: the first one is adheres to the standard, $N_p = 60$ and is shown in Fig. 1. The second arrangement consists of $N_p = 120$ pilots positioned as presented in Fig. 2, which is included for comparison with previous studies. It is important to point out that the pilot pattern in WiMAX differs from odd symbols to even symbols, as shown in Fig. 1. However, like [15], the proposed two-dimensional BEM can work with any pilot patterns. This offers a certain advantage over previous works on ICI mitigation. For the pilot schemes mentioned earlier, two different estimation matrices Γ were computed using (26) and (30): one was used to estimate channel weights for the even symbols ([odd even odd] pilot pattern) and the other one for the odd symbols ([even odd even]). The rest of the algorithm remains as explained in Section III.

Channel was implemented using the sum-of-sinusoids method explained in [22]. The channel power delay profile (PDP) consists of six uncorrelated paths defined by $p(\tau) = e^{-\frac{\tau}{\tau_0}} \delta(\tau - m\tau_0)$, $0 \leq \tau \leq 5\mu s$, $\tau_0 = 1\mu s$ and $m = (0, 1, \dots, 5)$;

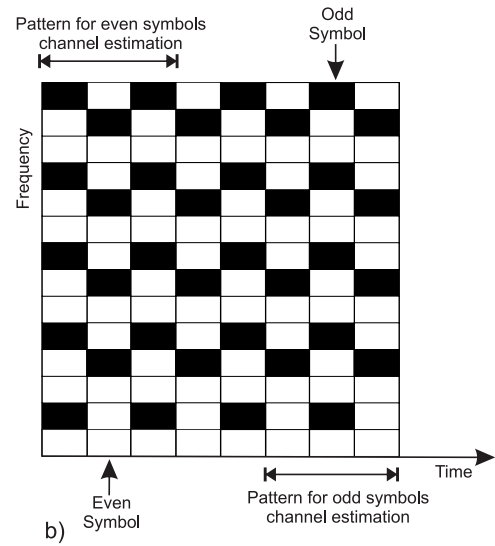


Fig. 2. Second pilot pattern. The black squares represent pilot subcarriers while the white squares represent data subcarriers. The proportion of pilot subcarriers is $2/7$ or $N_p = 120$ pilots.

TABLE III
CHANNEL POWER DELAY PROFILE

Path delay (μs)	0	1	2	3	4	5
Average power (dB)	0	-43	-86	-1.30	-1.73	-2.17

path delay and average power are shown in Table III. It should be pointed out that this PDP is equal to the one used in [11] and [8] in order to be consistent with the channel characteristics at comparison. According to the system sampling frequency F_s and with $\tau_{max} = 5\mu s$, the number of non-zero taps in the discrete CIR is $L = 29$.

The values for normalized Doppler frequencies f_D used in simulation are .1 and .2, which correspond to a transmission on a device at 436 km/h and 972 km/h of movement speed over a 2.4 Ghz carrier. It is important to point out that, since Doppler frequency is proportional to movement speed, result are equivalent for links with higher carrier frequencies and lower movement speeds. The metrics used for performance analysis are BER and the normalized mean squared error (NMSE), defined as:

$$NMSE = \frac{1}{M} \sum_{n=1}^M \frac{\sum_{k=1}^K \sum_{l=1}^L (\hat{h}_n(k, l) - h_n(k, l))^2}{\sum_{k=1}^K \sum_{l=1}^L (h_n(k, l))^2}, \quad (43)$$

where M is the number of transmitted symbols per run.

The number of basis functions per channel estimate considered in the simulation was computed using (11) and (17). This results in $Q = 26$ and $R_{ext} = \{2, 3, 4\}$. In practice, it is observed that in low interference (high SNR and/or low ICI), it is better to select a higher number of utilized functions in the time-Doppler domain to reduce the modeling error. Thus, when the iterative scheme is performed, the number of used functions R_{ext} was set to one more than the number provided by (17).

At the receiver, minimum mean square error (MMSE) equalization is performed after the mitigation of the ICI

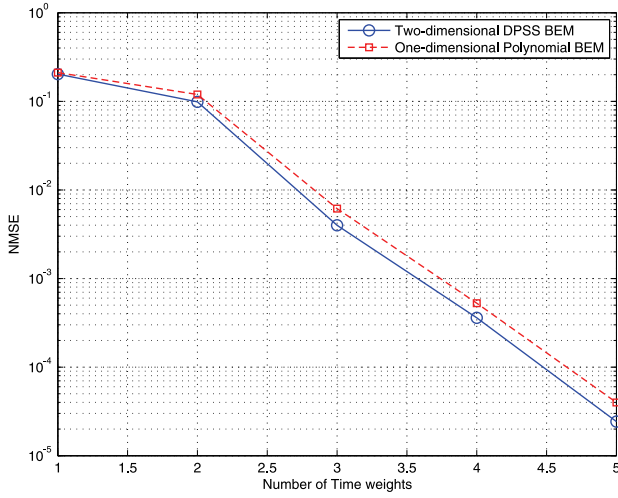


Fig. 3. Modeling error of the two-dimensional BEM for different numbers of time weights R_{ext} and one-dimensional time polynomial BEM for different numbers of polynomials. $Q = 27$, $L = 29$ and $f_D = .2$.

induced by pilots into the data subcarriers. Such equalization is performed in FD by using the QR-decomposition:

$$\hat{\mathbf{x}} = (\hat{\mathbf{G}}_d^H \mathbf{R}_w \hat{\mathbf{G}}_d + \mathbf{I})^{-1} \hat{\mathbf{G}}_d^H \mathbf{R}_w \hat{\mathbf{y}}_d \quad (44)$$

where $\hat{\mathbf{G}}_d$ is made up of the columns of the estimated channel matrix $\hat{\mathbf{G}}$ at data subcarrier positions and $\hat{\mathbf{y}}_d$ is a vector with the elements of \mathbf{y} at data positions after the removal of interference from the pilots.

Fig. 3 shows a comparison of modeling error when the two-dimensional DPSS BEM and the one-dimensional polynomial BEM are used for different numbers of time weights. Simulations were made considering $f_D = .2$. For the DPSS case, the number of time-delay weights Q was set at 27, while for the one-dimensional BEM every tap in the baseband channel model was expanded using the discrete Legendre orthogonal polynomials [23] as explained in [10]. It can be observed that in this case the modeling error of two-dimensional DPSS was slightly lower than the error obtained with the one-dimensional polynomial BEM. Note that even though both expanded the same process with similar performance, the two-dimensional BEM required fewer parameters ($Q = 27$ instead of $L = 29$).

Fig. 4 shows the NMSE estimator performance when different numbers of basis weights are set in both time and time-delay dimension. The conditions considered were $f_D = .1$ and $N_p = 60$ and no iterative scheme. The results show that the best performance is achieved when the number of weights satisfies (13) ($Q = 26$ and $R_{ext} = 3$). When any of these parameters increase, performance is diminished due to the increment of estimation error [24]. On the other hand, it can be noted that when a number of weights lower than that suggested by (17) and (11) is selected, the estimator performance falls somewhat since the modeling error increases [21].

Fig. 5 illustrates the NMSE of the proposed estimation algorithm for $f_D = .1$ with $N_p = 60$ pilots. The resulting curves correspond to performance when the iterative scheme has not been used (2D prolate no iterations), when one iteration is performed (2D prolate 1 iteration) and when the estimation considers that pilots do not have interference coming from

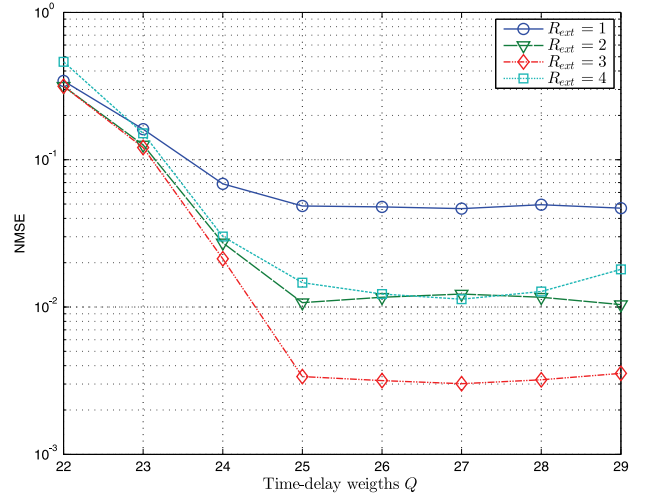


Fig. 4. Time-delay weights vs NMSE of the proposed estimation algorithm for different numbers of time weights R_{ext} , with no iterations, SNR= 25dB, $N_P = 60$ and $f_D = .1$.

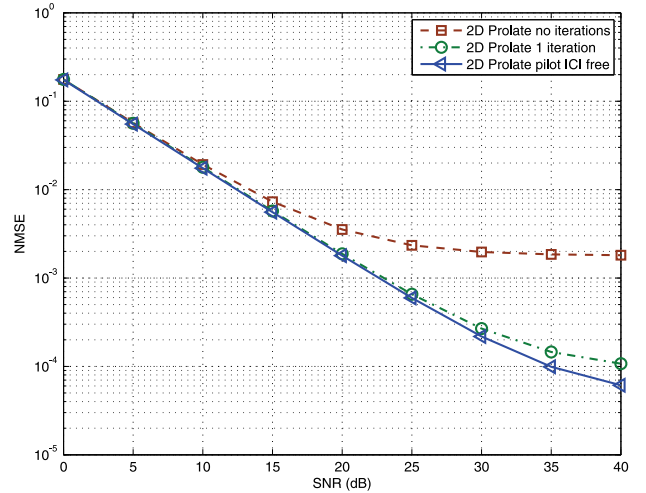


Fig. 5. SNR vs NMSE of the proposed estimation algorithm for $N_p = 60$, $I = QR = (26 * 3) = 78$ weights with no iterations and $I = QR = (26 * 4) = 104$ weights in the iterative scheme and pilot ICI-free. $f_D = .1$ equivalent to 437 Km/hr over a 2.4 Ghz carrier.

data subcarriers (2D prolate pilots ICI-free). When the pilots are free of data-ICI, the channel estimator operates with a transmitted OFDM symbol that contains training at pilots and zero values in data subcarriers. For the non-iterative scheme, $R_{ext} = 3$ was selected, while for the iterative case and ICI-free simulations $R_{ext} = 4$. From the curves, it is possible to observe that one iteration is enough to mitigate the distortion induced by the data-ICI.

Fig. 6 shows the BER in the environment considered above. The performance of the equalizer under perfect channel state information (CSI) conditions is included as a reference of the best BER achievable. Also, the estimator described in [15] was included for observing the performance of estimators that assume time-variability at frame level but omit ICI from intra-symbol variability. The figure shows that the proposed method under data-ICI free conditions achieves practically the same performance as the CSI case. This is the performance that can be expected from performing several iterations of the

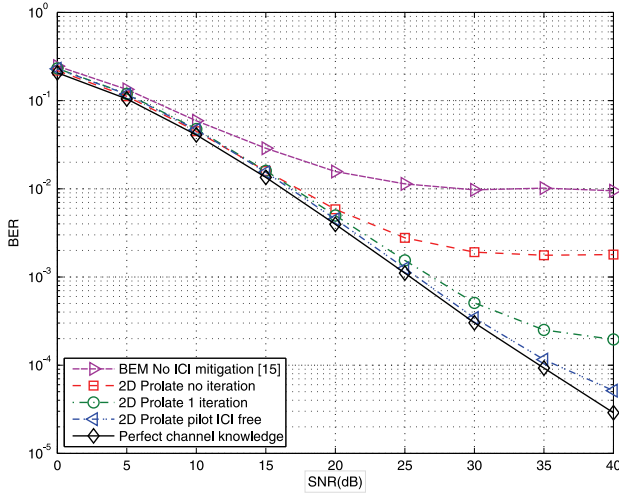


Fig. 6. SNR vs BER of the proposed estimation algorithm and the approach in [15] for $f_D = .1$ equivalent to 437 Km/hr over a 2.4 Ghz carrier. $N_p = 60$, $I = QR = (26 \times 3) = 78$ weights with no iterations and $I = QR = (26 \times 4) = 104$ weights in the iterative scheme and pilot ICI-free. Solid lines represent the performance obtained with CSI.

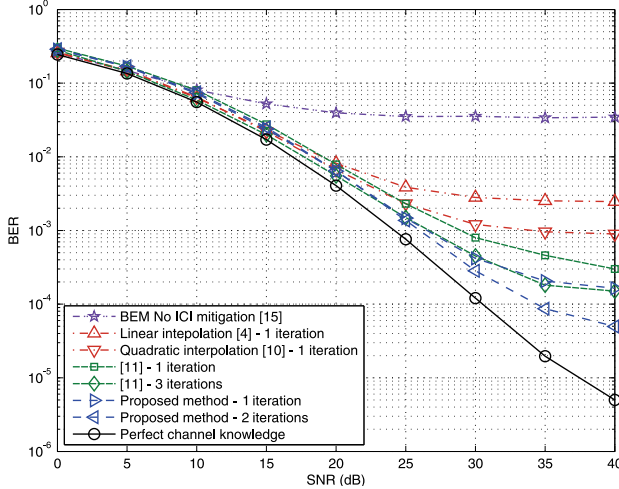


Fig. 7. SNR vs BER comparison of the proposed estimation algorithm and the methods in [4], [10], [11] and [15]. $N_p = 120$ pilots, $I = QR_{ext} = (26 \times 4) = 104$ weights and $f_D = .2$ equivalent to 874 Km/hr over a 2.4 Ghz carrier.

proposed algorithm. For SNR equal to or lower than 20 dB, the algorithm has BER near CSI even when no iterations are performed. For high SNR, one iteration provides a significant reduction of the BER compared with the non-iterative scheme (as much as ten times lower at SNR= 40 dB) approaching the performance of the CSI case. Note that the achieved performance when ICI is omitted is significantly lower than the one obtained when this phenomenon is included in the system model.

Fig. 7 presents a comparison among the BER obtained with the method introduced in [11] (because it provides the best reported performance results), interpolation methods in [4], [10] and the new approach presented in this paper. The cases of one and three iterations of [11] are denoted in the graph as [11] - 1 iteration and [11] - 3 iterations, respectively. For the interpolation methods, one iteration of lineal [4] and quadratic polynomials [10] are considered and

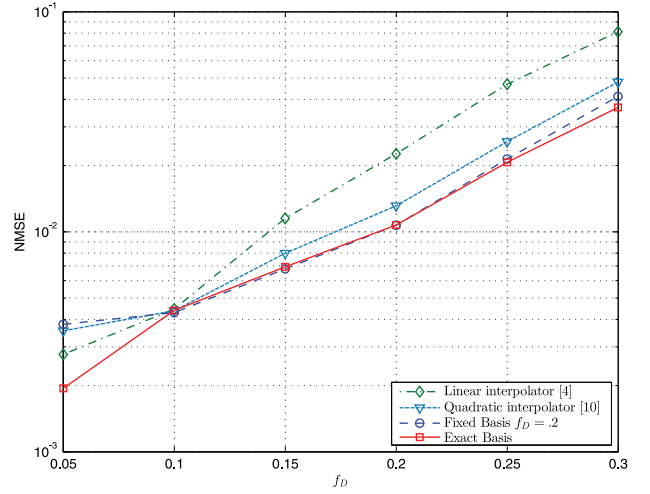


Fig. 8. f_D vs NMSE comparison of the proposed estimation algorithm and the methods in [11], [4] and [10] using $N_p = 120$ pilots.

denoted in the graph as [4] - 1 iteration and [10] - 1 iteration respectively. The proposed method considers one and two iterations (proposed method - 1 iteration and proposed method - 2 iterations). The simulations were performed using the second pilot arrangement $N_p = 120$. The results show that for an SNR below 20 dB, all the compared methods present a performance close to that achieved with CSI. For high SNR, it is possible to observe that the proposed algorithm with one iteration has a performance similar to that obtained with the method established in [11] with three iterations, and significantly better than [15], [4] and [10]. This result is remarkable considering the fact that the proposed algorithm has a computational complexity of $\mathcal{O}(N^2)$ while [11]'s is $\mathcal{O}(N^3)$. Even more, when two iterations are performed with the proposed algorithm, the BER is lower than 10^{-4} for SNR= 40dB, which could not be achieved by [11] using three iterations. Furthermore, all extra algorithms required by previous works for proper operation (path-delay estimations and a large number of FFTs) have been avoided, making the proposed approach a more robust solution.

In Fig. 8, the NMSE for different Doppler spreads and diverse algorithms is presented. For the two-dimensional DPSS BEM, two cases are considered: one with their basis and number computed according to each f_D , and a second case where the basis is constructed from the assumption of $f_D = .2$. The results show that the best performance is achieved when the bases are designed for each specific case. Nevertheless, it can be observed that similar results are obtained even though f_D considered in the basis construction is set at a fixed value. This characteristic is desirable because it implies robustness, i.e., the computed bases support different Doppler scenarios. In the case of low Doppler spread, similar performance is observed for all the algorithms considered in the graph.

VII. CONCLUSIONS

A low-complexity estimation algorithm for dealing with very fast time-varying channels was presented. Its performance in terms of BER is better than that of the state-of-the-art approaches requiring $\mathcal{O}(N^2)$ complex products. By

using an appropriate two-dimensional BEM, the only a priori information necessary to implement this algorithm is the maximum time-delay τ_{max} , the maximum Doppler frequency ν_{max} and the system parameters of effective bandwidth and symbol period. This makes the proposed algorithm feasible for implementation in practical applications. Furthermore, since the proposed algorithm works with any pilot pattern, current OFDM communication standards can use it; this would allow them to operate at higher mobility and/or higher carrier frequencies.

REFERENCES

- [1] P. Schniter, "Low-complexity equalization of OFDM in doubly selective channels," *IEEE Trans. Signal Process.*, vol. 52, no. 4, pp. 1002–1011, 2004.
- [2] A. Stamoulis, S. N. Diggavi, and N. Al-Dhahir, "Inter-carrier interference in MIMO OFDM," *IEEE Trans. Signal Process.*, vol. 50, no. 10, pp. 2451–2464, 2002.
- [3] T. Wang, J. G. Proakis, E. Masry, and J. R. Zeidler, "Performance degradation of OFDM systems due to Doppler spreading," *IEEE Trans. Wireless Commun.*, vol. 5, no. 6, pp. 1422–1432, 2006.
- [4] Y. Mostofi and D. C. Cox, "ICI mitigation for pilot-aided OFDM mobile systems," *IEEE Trans. Wireless Commun.*, vol. 4, no. 2, pp. 765–774, 2005.
- [5] H. M. Park and J. H. Lee, "Estimation of time-variant channels for OFDM systems using Kalman and Wiener filters," in *Proc. 2006 Vehicular Technology Conf. – Fall*, pp. 1–5.
- [6] K. Kwak, S. Lee, H. Min, S. Choi, and D. Hong, "New OFDM channel estimation with dual-ICI cancellation in highly mobile channel," *IEEE Trans. Wireless Commun.*, vol. 9, no. 10, pp. 3155–3165, 2010.
- [7] O. Simeone, Y. Bar-Ness, and U. Spagnolini, "Pilot-based channel estimation for OFDM systems by tracking the delay-subspace," *IEEE Trans. Wireless Commun.*, vol. 3, no. 1, pp. 315–325, 2004.
- [8] Z. Tang, R. C. Cannizzaro, G. Leus, and P. Banelli, "Pilot-assisted time-varying channel estimation for OFDM systems," *IEEE Trans. Signal Process.*, vol. 55, no. 5, pp. 2226–2238, 2007.
- [9] T. Hrycak, S. Das, G. Matz, and H. G. Feichtinger, "Practical estimation of rapidly varying channels for OFDM systems," *IEEE Trans. Commun.*, vol. 59, no. 11, pp. 3040–3048, 2011.
- [10] H. Hijazi and L. Ros, "Polynomial estimation of time-varying multipath gains with inter-carrier interference mitigation in OFDM systems," *IEEE Trans. Veh. Technol.*, vol. 58, no. 1, pp. 140–151, 2009.
- [11] —, "Joint data QR-detection and Kalman estimation for OFDM time-varying Rayleigh channel complex gains," *IEEE Trans. Commun.*, vol. 58, no. 1, pp. 170–178, 2010.
- [12] J. Ma, P. Orlik, J. Zhang, and G. Y. Li, "Statistics-based ICI mitigation in OFDM over high-mobility channels with line-of-sight components," *IEEE Trans. Wireless Commun.*, vol. 10, no. 11, pp. 3577–3582, 2011.
- [13] R. Carrasco-Alvarez, R. Parra-Michel, A. G. Orozco-Lugo, and J. K. Tugnait, "Time-varying channel estimation using two-dimensional channel orthogonalization and superimposed training," *IEEE Trans. Signal Process.*, vol. 60, no. 8, pp. 4439–4443, 2012.
- [14] O. Longoria-Gandara and R. Parra-Michel, "Estimation of correlated MIMO channels using partial channel state information and DPSS," *IEEE Trans. Wireless Commun.*, vol. 10, no. 11, pp. 3711–3719, 2011.
- [15] P. Salvo Rossi and R. R. Muller, "Slepian-based two-dimensional estimation of time-frequency variant MIMO-OFDM channels," *IEEE Signal Process. Lett.*, vol. 15, pp. 21–24, 2008.
- [16] T. Zemen, L. Bernado, N. Czink, and A. F. Molisch, "Iterative time-variant channel estimation for 802.11p using generalized discrete prolate spheroidal sequences," *IEEE Trans. Veh. Technol.*, vol. 61, no. 3, pp. 1222–1233, 2012.
- [17] P. S. Rossi, R. R. Miller, and O. Edfors, "Linear MMSE estimation of time-frequency variant channels for MIMO-OFDM systems," *Signal Process.*, vol. 91, no. 5, pp. 1157–1167, 2011. Available: <http://www.sciencedirect.com/science/article/pii/S0165168410004068>
- [18] V. Kontorovich, S. Primak, A. Alcocer-Ochoa, and R. Parra-Michel, "MIMO channel orthogonalizations applying universal eigenbasis," *IET Signal Process.*, vol. 2, no. 2, pp. 87–96, 2008.
- [19] D. Slepian, "Prolate spheroidal wave functions, fourier analysis, and uncertainty-IV: extensions to many dimensions; generalized prolate spheroidal functions," *Bell Syst. Tech. J.*, vol. 43, pp. 3009–3058, 1964.
- [20] S. M. K. Dimitris G. Manolakis, and Vinay K. Ingle, *Statistical and Adaptive Signal Processing: Spectral Estimation, Signal Modeling, Adaptive Filtering, and Array Processing*. McGraw-Hill, 2000.
- [21] H. L. V. Trees, *Detection, Estimation, and Modulation Theory, Part I*. Wiley-Interscience, 2001.
- [22] Y. R. Zheng and C. Xiao, "Simulation models with correct statistical properties for Rayleigh fading channels," *IEEE Trans. Commun.*, vol. 51, no. 6, pp. 920–928, 2003.
- [23] E. Brookner, *Tracking and Kalman Filtering Made Easy*. John Wiley & Sons, 1998.
- [24] S. M. Kay, *Fundamentals of Statistical Signal Processing, Volume I: Estimation Theory*. Prentice-Hall Signal Processing Series, 1993, vol. I.



F. Peña-Campos was born in Guadalajara City, Mexico, in 1986. In 2008, he received the B.Sc. degree in electronics and communications from University of Guadalajara, Jalisco, Mexico, and in 2011 the M.Sc. degree in electrical engineering, specializing in communications, from CINVESTAV-IPN, Guadalajara, Mexico, where he is currently working toward the Ph.D. degree. His research interests include digital signal processing, modeling, characterization and estimation of wireless channels.



Roberto Carrasco-Alvarez was born in Mexico City, Mexico, in 1981. He received the B.Sc. degree in electronics from Instituto Tecnológico de Morelia, Morelia, Michoacan, Mexico, in 2004, the M.Sc. and Ph.D. degrees in electrical engineering, specializing in telecommunications, from CINVESTAV-IPN, Guadalajara, Mexico, in 2006 and 2010 respectively. He currently is professor and researcher in CUCEL, Universidad de Guadalajara. His research interests include signal processing and digital communications.



O. Longoria-Gandara was born in Delicias, Mexico, in 1971. He received a B.Sc. degree in electronics and communications from the Instituto Tecnológico y de Estudios Superiores de Monterrey (ITESM-Mty.) in 1993; the M.Sc. degree in electrical engineering specialized in communications from CINVESTAV-IPN, Mexico, in 1998. From 1998 to 2006 he was with the Electrical Engineering Department (EED) of ITESM-Guadalajara as full time Professor and from 2004 to 2006 he was in charge of this department. In the summer of 2001 and 2002 he received a Project Orient Learning seminar at Twente University in Netherlands which result was the publishing of a Hardware Computer Design Handbook for the ITESM. Since 2001 he has been a committee member of the General Electric Foundation scholarships for Mexico. He received the PhD degree in 2010 at CINVESTAV-IPN, Guadalajara, Mexico, where he has done research in time invariant/variant MIMO channel estimation, radio channel modeling and space-time block codes. His research interests include MIMO channel estimation, MIMO digital precoding and implementation of embedded communications algorithms using hardware description languages. Currently, he is with the Electronics, Systems and Computer Department at ITESO University, Mexico, and he is cooperating with CINVESTAV, Gdl. and Intel-Labs Guadalajara, Mexico.



Ramon Parra-Michel (S97M04) was born in Guadalajara City, Mexico, in 1973. He received the B.Sc. degree in electronics and communications from University of Guadalajara, Jalisco, Mexico, in 1996, the M.Sc. degree in electrical engineering, specializing in communications, from CINVESTAV-IPN, Guadalajara, Mexico, in 1998 and the Ph.D. degree in electrical engineering specialized in digital signal processing for communications from CINVESTAV-IPN, Mexico City, in 2003. He has collaborated with several companies and institutions either in academic or technology projects, such as Siemens, Lucent, Mabe, Mixbaal, Hewlett-Packard and Intel. He is currently a full member of research staff at CINVESTAV-IPN in Guadalajara Unit. His research interests include modeling, simulation, estimation and equalization of communication channels, and digital implementation of DSP algorithms for communication systems.